Chinese Chemical Letters 36 (2025) 110028

Contents lists available at ScienceDirect

Chinese Chemical Letters

journal homepage: www.elsevier.com/locate/cclet

Low-dimensional antimicrobial nanomaterials in anti-infection treatment and wound healing

Yunfen Gao[a,1], Liying Wang[b,1], Chufan Zhou[c], Yi Zhao[a,*], Hai Huang[d,*], Jun Wu[e,f,*]

[a] School of Biomedical Engineering, Shenzhen Campus of Sun Yat-sen University, Shenzhen 518107, China
[b] Department of Hematology, The Seventh Affiliated Hospital, Sun Yat-sen University, Shenzhen 518107, China
[c] School of Life Sciences and Bio-pharmaceutics, Guangdong Pharmaceutics University, Guangzhou 510006, China
[d] Department of Urology, Sun Yat-sen Memorial Hospital, Sun Yat-sen University, Guangzhou 510120, China
[e] Bioscience and Biomedical Engineering Thrust, The Hong Kong University of Science and Technology (Guangzhou), Nansha, Guangzhou 511400, China
[f] Division of Life Science, The Hong Kong University of Science and Technology, Hong Kong SAR 999077, China

ARTICLE INFO

Article history:
Received 5 April 2024
Revised 14 May 2024
Accepted 17 May 2024
Available online 18 May 2024

Keywords:
Nano-antimicrobial materials
Antimicrobial mechanisms
Low-dimensional
Anti-infection treatment
Wound healing

ABSTRACT

Bacterial infections have always been a major threat to human health. Skin wounds are frequently exposed to the external environment, and they may become contaminated by bacteria derived from the surrounding skin, the local environment, and the patient's own endogenous sources. Contaminated wounds may enter a state of chronic inflammation that impedes healing. Urgent development of antibacterial wound dressings capable of effectively combating bacteria and overcoming resistance is necessary. Nanotechnology and nanomaterials present promising potential as innovative strategies for antimicrobial wound dressings, owing to their robust antibacterial characteristics and the inherent advantage of avoiding antibiotic resistance. Therefore, this review provides a concise overview of the antimicrobial mechanisms exhibited by low-dimensional nanomaterials. It further categorizes common low-dimensional antimicrobial nanomaterials into zero-dimensional (0D), one-dimensional (1D) and two-dimensional (2D) nanomaterials based on their structural characteristics, and gives a detailed compendium of the latest research advances and applications of different low-dimensional antimicrobial nanomaterials in wound healing, which could be helpful for the development of more effective wound dressings.

1. Introduction

Bacterial infections have always posed a significant threat to human health. Due to its extensive surface area, the skin is susceptible to easy injury, and subsequent wounds may become contaminated by bacteria originating from the surrounding skin, local environment, and endogenous microflora of the patient. The infection process can be summarized as contamination, colonization, critical colonization, and ultimately successful infection [1]. The colonization stage is defined as the presence of proliferating bacteria in a wound that has been contaminated with bacteria without an apparent host response. Wounds in the critical colonization stage may enter a non-healing chronic inflammatory state [2]. The transition to infection occurs when bacterial proliferation overcomes the host immune response and results in host damage [3]. Studies have shown that *Staphylococcus aureus* (*S. aureus*) and coagulase-negative *Staphylococcus* are common colonizing flora in chronic wounds, with an increase in types of colonizing flora observed as wound non-healing time prolongs [2]. Therefore, timely administration of effective antibacterial agents is crucial for promoting wound healing. Currently, various forms of wound dressings incorporate antibiotics, nanoparticles, cationic organic agents, *etc*., serving as antibacterial agents [3-6]. Over the past few decades, antibiotics have been the primary treatment for bacterial infections [7-9]. Since Alexander Fleming's discovery of penicillin in 1928 and its subsequent use for treating bacterial infections starting from 1940 until now, antibiotics' potent effect on bacterial infections has earned them the reputation of being life-saving "Wonder Medicine" they truly are [10]. The discovery of antibiotics has saved countless lives. However, researchers soon discovered bacteria's resistance to antibiotics, such as widespread resistance among *Escherichia coli* (*E. coli*) strains to fluoroquinolone antibiotics [11-13]. In many parts of the world today, more than half of patients are unresponsive to this treatment option [9]. Some studies have conducted DNA-targeted metagenomic analysis of 30,000-year-old

* Corresponding authors.
E-mail addresses: zhaoy529@mail.sysu.edu.cn (Y. Zhao), huangh9@mail.sysu.edu.cn (H. Huang), junwuhkust@ust.hk (J. Wu).
[1] These authors contributed equally to this work.

https://doi.org/10.1016/j.cclet.2024.110028
1001-8417/

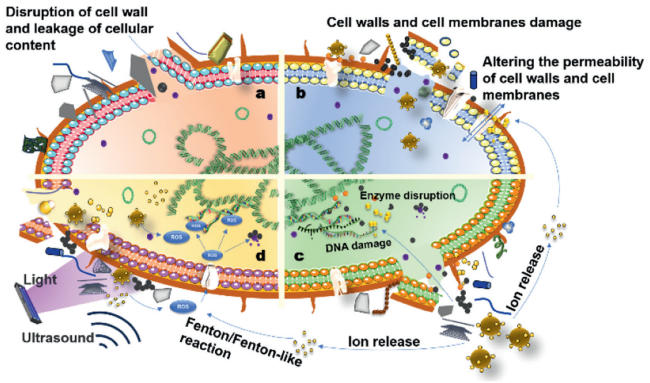

Fig. 1. Different antimicrobial mechanisms of nanomaterials.

Bering permafrost sediments. The findings indicate that antibiotic resistance is an inherent phenomenon predating the contemporary selection pressure exerted by clinical antibiotic usage [14]. In essence, antimicrobial resistance (AMR) poses a global threat to health and development [15-17]. The World Health Organization (WHO) has identified AMR as one of the ten major public health threats facing humanity [9].

In recent years, nanomaterials have made significant strides in the realm of antibacterial applications. Antimicrobial nanomaterials are rapidly advancing, with research focusing on various materials such as inorganic carbon materials, metals/metal oxides, organic liposomes, and polymeric nanomaterials for nano-antimicrobials [18,19]. These types of antimicrobial nanoparticles and nanoscale antibiotic delivery vehicles have demonstrated their efficacy *in vitro* and animal models for treating infectious wounds including those caused by antibiotic-resistant diseases [20,21]. However, there is currently no comprehensive review available on the latest application of low-dimensional nanomaterials in wound healing. Therefore, this review provides a concise summary of the antimicrobial mechanisms exhibited by different nanomaterials while offering an extensive compilation of recent research progress and applications pertaining to various low-dimensional antimicrobial nanomaterials used in wound healing. This endeavor aims to facilitate the development of more effective antimicrobial wound dressings.

2. Antimicrobial mechanisms of nanomaterials

The basic structures of bacteria include cell walls, cell membranes, nucleus-like nuclei, and cytoplasm containing ribosomes and plasmids. For different bacterial structures, the antimicrobial effect of nanomaterials exhibits diverse mechanistic pathways (Fig. 1) [22]. The shape and size of nanomaterials are important factors affecting their antibacterial activity. On the one hand, antibacterial nanomaterials can kill bacteria by destroying cell walls and cell membranes, and on the other hand, once nano-materials penetrate into the interior of bacteria, they can perturb normal functional metabolism through ion release, generation of reactive oxygen species (ROS), *etc*. [23]. Herein, based on the process from external to internal microbial damage, we categorize the antibacterial mechanism of low-dimensional nanomaterials into four parts: physical contact cutting damage, interaction with the cell membrane causing membrane damage, internal structure impairment, and ROS release for antimicrobial action. Most antimicrobial materials exhibit interconnected mechanisms rather than independent ones; often a synergistic effect from multiple mechanisms contributes to effective antimicrobial activity [24].

2.1. Physical destruction

The initial step in the antimicrobial activity of nanomaterials involves complete contact with microorganisms. The cell wall serves as a stress barrier for microorganisms preventing mechanical harm that could lead to osmotic rupture while maintaining their structural integrity [25]. Due to their sharp lamellar structure, two-dimensional (2D) nanomaterials possess unique physical bactericidal capabilities. When 2D nanomaterials come into contact with bacterial surfaces, the edges act like nano-knives, cutting directly into the bacterial membrane structure, resulting in bacterial rupture and leakage of cytoplasm. This ultimately leads to bacterial death [26]. In addition to the typical blade-shaped 2D nanomaterials, cluster-shaped or flower-shaped nanomaterials resemble a combination of spears that can penetrate the external structure of bacteria, leading to bacterial rupture and death. A study conducted by Talebian *et al.* investigated the impact of ZnO nanoparticles (ZnO NPs) morphology on their antibacterial properties, revealing that flower-type ZnO NPs with sharp structures exhibited superior bactericidal effects compared to smooth nanorods [27]. The physical cutting damage caused by this morphology often serves as the initial step in nanomaterial sterilization, followed by further induction of sterilization function after cell membrane incision [28].

2.2. Cell membrane damage

The negative charge on the surface of the bacterial cell wall facilitates strong adhesion of positively charged nanomaterials such as AgNPs and Al_2O_3. Nanomaterials can tightly adhere to the bacterial cell membrane through physical diffusion and electrostatic adsorption [29,30]. Once attached to the bacterial surface, antibacterial nanomaterials can alter the permeability of the cell membrane and disrupt its physiological metabolism by damaging surface proteins and other bioactive components of the bacterial cell membrane. Metal nanoparticles attach to sulfur or phosphorus-containing proteins on the surface of the bacterial wall/cell membrane, leading to depressions on bacteria surfaces and causing irreversible damage to their walls/membranes [31]. Hydroxyl groups on SiO_2 nanoparticles interact with polysaccharides on *E. coli* surfaces, resulting in disruption of the cell membrane [32]. Furthermore, nanomaterials exhibit a higher rate of ion leaching compared to larger-sized materials. Kügler *et al.* proposed an "ion exchange mechanism" that induces bacterial death: charges are exchanged between cationic polymer surfaces and divalent cations (Mg^{2+} and Ca^{2+}) in bacterial cell walls, depleting divalent from these walls which subsequently loosen and disintegrate [33]. Many metal ions also alter ion permeability in bacterial cell membranes, affecting material transport capabilities as well as material storage capacities within these membranes [34]. Silver ions have been observed reacting with thiols and amino groups present in enzymes on bacterial membrane surfaces, thereby influencing transmembrane ion transport functions [35]. AgNPs can also interact with peptidoglycan cell walls in bacteria, increasing membrane permeability while altering osmotic pressures within these membranes ultimately leading to bactericidal effects [36].

The formation of biofilms is a significant impediment to the treatment of bacterial infections [37]. Quorum sensing (QS) serves as a vital mechanism for internal recognition, communication, and gene expression control in bacteria, playing a crucial role in biofilm formation. Therefore, QS inhibition represents an important novel antibacterial strategy against biofilm-forming bacteria. By disrupting QS transmission, inhibiting toxic intercellular communication among bacteria, and preventing bacterial biofilm formation, QS inhibition can effectively impede the progression of bacterial infections [38,39]. Small-sized metal nanomaterials such as AgNPs can penetrate bacterial biofilms, reduce the expression of extracellu-

lar polysaccharides and QS-dependent related factors, inhibit microbial QS, and thereby inhibit the formation of biofilms [40,41].

2.3. Internal structural damage

In addition to focusing on protein dysfunction and membrane damage in cell membranes, nanoantibacterial agents also possess molecular antibacterial effects that enable them to penetrate bacterial walls and membranes, reacting with proteins, enzymes, and other substances inside the cells to render them inactive [42]. For instance, metal nanoparticles can interact non-covalently with DNA and RNA in bacteria and fungi through non-covalent interactions, altering the secondary conformation of DNA and RNA structures. This leads to the separation of the DNA double helix, interfering with the expression of related proteins and disrupting the process of DNA replication [29,43]. Photothermal therapy (PTT) based on photothermal agents (PTAs) has the ability to convert light into heat. The generated heat irreversibly denatures proteins present in cell membranes and cytoplasm, resulting in an effective antimicrobial effect [33,44].

2.4. Oxidative stress damage

ROS refers to highly reactive free radical substances associated with oxygen metabolism in living organisms, including peroxides (H_2O_2), superoxide ($O_2^{\bullet-}$), hydroxyl radicals ($^{\bullet}OH$), and monoclinic oxygen ($^1O_2$). The oxidative stress caused by ROS can rapidly oxidize and destroy essential biomolecules such as bacterial nucleic acids, membrane lipids, and proteins. Therefore, the level of ROS directly correlates with the antibacterial activity of materials [45,46]. Antimicrobial agents utilizing ROS exhibit high precision and exceptional bactericidal ability, making it an effective strategy against AMR [47,48]. Different nanomaterials respond differently to external stimuli. Common antibacterial strategies of metal and metal oxide nanoparticles, carbon-based materials and photosensitive polymers are all based on ROS stimulus-response strategies to achieve antibacterial activity [49-51]. Zhang *et al.* compared the ROS antimicrobial activities of silver, gold, nickel, and silicon nanoparticles and found that AgNPs could simultaneously induce the generation of superoxide ($O_2^{\bullet-}$) and hydroxyl radical ($^{\bullet}OH$), exhibiting the highest ROS antimicrobial performance [52]. Graphene materials possess excellent photothermal properties which are widely utilized in photothermal antimicrobial therapy. Exposure to graphene/graphene-like materials significantly increased intracellular levels of ROS in *E. coli* strains [53].

3. Zero-dimensional antimicrobial nanomaterials

3.1. Nano metal-based antimicrobial materials

According to the conventional definition, nanomaterials are classified into 0D, 1D, and 2D based on their dimensions in the *x*, *y*, and *z* directions. 0D materials refer to nanomaterials with sizes smaller than 100 nm in all three dimensions, such as nanoparticles, nanoflowers, and nanoclusters [54,55]. Being one of the earliest forms of nanomaterials, nanoparticles possess remarkable properties including low toxicity and antimicrobial effects due to their small size and high specific surface area. These characteristics enable them to access hard-to-reach areas for bulky molecules while facilitating diffusion and internalization by bacteria [56]. Moreover, metal nanoparticles have been extensively utilized in biotechnology, nanomedicine, and biopharmaceutical fields for antibacterial applications owing to their exceptional ability to enhance the efficacy of various drugs [57-60].

Silver nanoparticles (AgNPs) are currently the most widely used nano antibacterial metal materials in wound healing [61,62]. The specific antibacterial activity of AgNPs is attributed to the fusion of metal ions with bacterial enzyme systems upon release and oxidative stress induced by ROS on their surface [63-65]. Ma *et al.* extracted water-soluble polysaccharides from *Astragalus* root (AMWP) and successfully synthesized spherical AgNPs mediated by AMWP (AMWP-AgNPs), which had an average diameter of 65.08 nm [66]. Evaluation of the prepared AMWP-AgNPs against four clinically isolated multi-drug resistant (MDR) bacteria demonstrated significant inhibition of drug-resistant strains at low concentrations, indicating great potential for future applications in combating MDR bacteria. Malik *et al.* employed a green one-pot method to synthesize AgNPs and incorporated them into hydrogels to confer antibacterial activity on hydrogel dressings. However, the relatively low mechanical properties of bio-based hydrogels limit their use as load-bearing scaffolds. To address this issue, they introduced 2D layered graphitic carbon nitride (g-C_3N_4) into hydrogels to obtain nanocomposite hydrogel membranes with improved mechanical properties [67]. The addition of g-C_3N_4 not only enhances the mechanical properties but also imparts superior antibacterial characteristics to the hydrogel. Zhou *et al.* developed a novel multifunctional platform (Alg/1.0Ag@CMC-PAMAM/PRP) by incorporating nano-silver-doped sodium alginate-based dressings mixed with platelet-rich plasma (PRP) as a wound dressing [68]. The presence of Ag@CMC-PAMAM nanoparticles in this composite dressing confers excellent antibacterial properties, while the incorporation of PRP regulates the expression of relevant active factors to promote anti-inflammatory responses and angiogenesis for inflammation inhibition purposes. The characterization revealed that this dressing exhibits excellent swelling properties, a suitable water vapor transmission rate (WVTR), favorable mechanical properties, degradability, and sustained release of PRP. This study demonstrates the promising potential of the prepared Alg/1.0Ag@CMC-PAMAM/PRP in the field of biomedicine due to its antibacterial and wound-healing effects.

In addition to conventional sheet and gel wound dressings, sprayable antibacterial wound dressings serve as alternative options. Compared to dressings with a relatively simplistic structure, sprayable dressings offer the advantages of controllable shape and dosage, enhanced permeability, and the ability to reach inaccessible wound gaps for promoting effective wound healing. Amirsadeghi *et al.* developed a novel sprayable antibacterial dressing by combining Persian gum (PG) with AgNPs, which was then sprayed onto wounds to form a complete film for coverage [69]. The antibacterial evaluation demonstrated that 1% PG/AgNPs exhibited bactericidal activity against *Pseudomonas aeruginosa* and *S. aureus*. The evaluation of cytotoxicity and *in vivo* assessment of full-thickness wound healing confirmed the safety and efficacy of a 1% PG/AgNPs spray, demonstrating its significant potential for enhancing the wound repair process.

Studies have demonstrated the potential of metal nanoclusters, such as Ag, Au, and Au-Ag nanoclusters, with a size smaller than 2 nm as effective antibacterial materials. One reason for their efficacy is their ability to easily diffuse and be internalized by bacteria. Additionally, these metal nanoclusters can elevate the level of ROS in local wounds, thereby enhancing the antibacterial efficiency of nanoparticles [70-72]. Zhou *et al.* utilized gold nanoparticles (AuNPs) to amplify the antibacterial effect of gentamicin sulfate (GM) and precisely load it onto a woven silk fabric (SF) wound dressing in order to reduce dosage during wound treatment [73]. The findings reveal that this novel dressing fabric (SF@Au/GM) exhibits significantly enhanced antibacterial properties even at lower gentamicin concentrations. Furthermore, this composite SF pad demonstrates favorable biocompatibility and applicability as a wound dressing material. Animal experiments have indicated that on the 15th day of treatment, SF@Au/GM displays superior cell appendages and epidermal growth compared to Aquacel Ag®, a com-

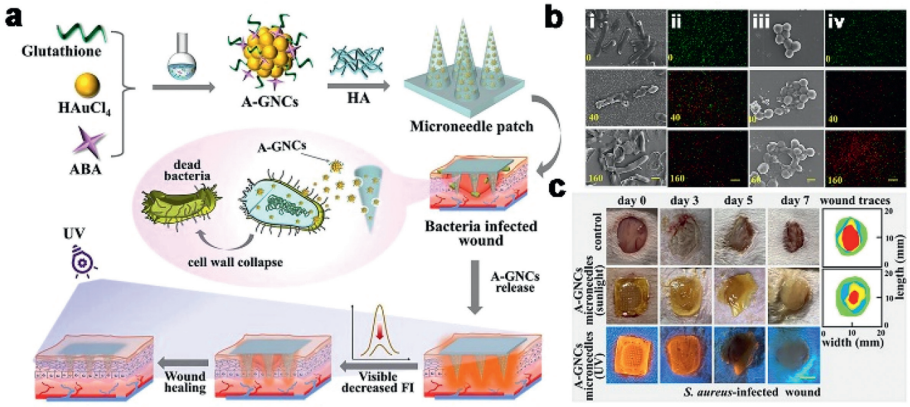

Fig. 2. (a) Schematic illustration of A-GNCs encapsulated fluorescent microneedles array. (b) Antibacterial properties of A-GNCs microneedles. (c) A-GNCs microneedle patches treat infected skin wound models on rats. The scale bars are 600 nm in b(i) and b(iii), and 50 μm in b(ii) and b(iv). Copied with permission [75]. Copyright 2024, Wiley.

mercial wound dressing product. Therefore, this innovative type of dressing fabric (SF@Au/GM) holds promise for use in wound repair procedures while offering a potential solution for mitigating antibiotic overuse. Conventional antimicrobial strategies often fall short in achieving desired outcomes against super bacteria. Zou *et al.* incorporated AuNPs into gentamicin sulfate (GS) and loaded them into a blend of konjac glucomannan (KGM) and gelatin to create a wound dressing known as KGM/Gelatin@AuNPs/GS [74]. The antibacterial experiment demonstrated that the presence of AuNPs enhanced the antimicrobial activity of gentamicin sulfate; the composite dressing effectively eradicated bacteria, including super bacteria. Recently, Yi *et al.* reported a novel transdermal antimicrobial microneedle patch consisting of hyaluronic acid (HA) encapsulated gold nanoclusters (A-GNCs) (Fig. 2a) [75]. The photoluminescent properties of GNCs allowed for bright fluorescence emission under ultraviolet (UV) light, enabling monitoring of the remaining dose of A-GNCs. It can be observed that the introduction of A-GNCs led to collapse and fusion of bacterial cell walls (Fig. 2b), while in a rat-infected skin wound model, these patches exhibited excellent therapeutic efficacy against microbial infections (Fig. 2c).

Zinc serves as a vital cofactor for metalloproteins and plays a crucial role in the regeneration process of the extracellular matrix [76,77]. Moreover, zinc also functions as a regulator for automatic debridement and keratinocyte migration, both of which are indispensable for wound repair [78]. Wounds deficient in zinc typically exhibit delayed healing [77]. The delivery method of zinc is crucial for achieving the beneficial healing effects of zinc [79]. Hydrated zinc oxide exhibits high sensitivity to phosphate ions at pH 7, resulting in the degradation of ZnO NPs and stable release of zinc ions [80]. ZnO NPs serve as a continuous source of zinc ions, making them suitable for local wound application by promoting re-epithelialization, reducing inflammation, and inhibiting bacterial growth [81]. Rath *et al.* prepared ZnO NPs using the zinc chloride reduction method and fabricated a composite nanofibrous pad containing both zinc oxide and cefazolin by electrostatic spinning onto gelatin fibers [78]. Their research demonstrated that compared to regular cefazolin or ZnO NPs-loaded pads, the compounded drug-containing nanofiber pads exhibited accelerated wound healing. When the weight ratio of ZnO NPs to cefazolin was 1:1, the gelatin composite fiber mat displayed an antibacterial activity level of 1.9 ± 0.2 μg/mL. Macroscopic and histological evaluations revealed that ZnO NPs hybridized with cefazolin nanofibers enhanced cell adhesion and epithelial migration, leading to faster and more efficient collagen synthesis. Therefore, this manufactured composite nanofiber pad may be utilized as an antibacterial wound dressing post-surgery.

Bužarovska *et al.* fabricated a thermally induced phase separation (TIPS) derived thermoplastic polyurethane (TPU)/ZnO nanocomposite foam [82]. The highly porous structure of this composite foam consists of interconnected pores ranging in size from 10 μm to 60 μm, as observed by scanning electron microscopy (SEM). The results demonstrate an impressive water vapor transmission rate (WVTR) of up to 8.9 mg cm^{-2} h . When evaluating the cell-supporting capability and growth potential, TPU nanocomposite foams containing 2 and 5 wt.% ZnO exhibited the highest cell proliferation rates, indicating excellent biocompatibility and low cytotoxicity. Therefore, this TPU/ZnO nanocomposite foam holds promise as an active wound dressing material for biomedical applications. Haider *et al.* employed alkali lignin as a reducing agent to synthesize CuO nanoparticles on the surface of electrospun cellulose (CE) nanofibers [83]. This Cu/CE nanofiber releases approximately 80% of copper ions into the surrounding water environment within a span of 24 h, with subsequent stabilization over the following five days. Notably, the Cu/CE nanofiber mat exhibits remarkable antibacterial effects against both Gram-negative *E. coli* and Gram-positive *S. aureus* strains, while promoting excellent migration and proliferation capabilities in NIH3T3 fibroblasts residing within the fiber matting structure. These findings highlight the potential utilization of such nanofiber pads as wound dressing materials.

3.2. Carbon dots (CDs)

CDs are nanomaterials with a *quasi*-spherical morphology and small particle size (<10 nm), composed of elemental carbon. Since their discovery in 2004, CDs have garnered significant attention in the fields of biomedical and energy applications [84,85]. Over the past two decades, extensive research has been conducted on CDs, leading to their classification as graphene or carbon quantum dots (CQDs), carbon nanodots (CNDs), and carbon-copolymer dots (CPDs) based on variations in their fluorescence mechanisms [86-89]. In the absence of light excitation, CDs can adhere to bacterial cell walls through electrostatic interactions, disrupting their physiological metabolism and propagation. Moreover, due to their extremely small size, CDs can infiltrate bacterial walls and membranes, causing damage to intracellular structures and exhibiting antibacterial effects [90-93]. Numerous biomedical antimicrobial applications have been developed over the last twenty years by synthesizing functionalized carbon dots using various methods and raw materials [94-96].

The degradable carbon dots prepared by Zhao *et al.* can be completely degraded into CO_2, CO and H_2O within 20 days at 37 °C. They exhibit potent broad-spectrum antibacterial activity, effec-

tively inhibiting the growth of various bacteria and fungi such as *S. aureus*, *Bacillus subtilis*, *Bacillus spp.*, *E. coli* (including ampicillin-resistant strains), *Fusarium solanacearum*, and *Botrytis cinerea* [97]. Hydrogel dressings have been extensively investigated for wound healing applications. Cui *et al.* developed a biocompatible adherent antimicrobial cationic CDs hydrogel with excellent adhesion by incorporating carbon dots containing spermidine and lipoic acid prepared through a one-pot method into a hydrogel network formed *via* ester bond formation between polyacrylic acid and pectin [98]. When bacteria come into contact with the hydrogel, the equilibrium of hydrogen bonds between CDs, polyacrylic acid, and pectin is disrupted, leading to the release of CDs that exhibit bactericidal activity and provide protection against bacterial infection for the wound. The CDs synthesized in Wang *et al.*'s study can even induce the epithelial-mesenchymal transition (EMT) process by activating the transforming growth factor-β/p38 mitogen-activated kinase/Snail signaling pathway, promoting cell migration and accelerating wound repair. The multifunctional wound healing system doped with CQDs developed by Zheng *et al.* added phenol red and CQDs [99]. The addition of phenol red and CQDs imparted high sensitivity to pH changes in the wound environment. This sensitive colorimetric and fluorescence-responsive system enables real-time monitoring of wound status while also exhibiting excellent antibacterial properties to facilitate wound repair.

4. One-dimensional (1D) antimicrobial nanomaterials

In addition to conventional nanoparticles, there is a growing trend towards the development of 1D nanoantibacterial materials. 1D nanomaterials refer to nanomaterials with one dimension larger than 100 nm, significantly surpassing the size of another dimension [100]. Distinguished from singular nanoparticles, the unique structure of 1D nanoparticles endows them with excellent mechanical properties. The incorporation of 1D nanomaterials can enhance the thermal stability of materials, and their exceptional flexibility and mechanical strength are particularly crucial in wound dressing applications [7,101]. Currently, metal nanowires, nanorods, as well as carbon-based nanomaterials like carbon nanotubes (CNTs) and carbon-based nanowires (CNFs) are among the most commonly used types of 1D antimicrobial materials [84,102].

4.1. Carbon-based 1D nanomaterials

Md Shahidul Islam *et al.* utilized electrospinning technology to fabricate a polyvinyl alcohol (PVA) nanofiber mat with uniformly distributed AgNPs and carbon nanotubes (CNTs) [103]. At a specific content ratio, AgNPs and CNTs can be evenly precipitated onto the PVA electrospun fiber mat without altering its surface morphology. Characterization of this multi-composite nanofiber mat revealed that the incorporation of CNTs enhances its tensile strength, while the addition of AgNPs and CNTs improves its thermal stability. Moreover, due to the synergistic effect between AgNPs and CNTs, the antibacterial activity of the composite nanofiber mat is significantly enhanced. However, it should be noted that achieving optimal dispersion often comes at the expense of nanoparticle size distribution. Zhu *et al.*, on the other hand, employed encapsulation techniques to coat single-walled carbon nanotubes (SWCNTs) with AgNPs and mesoporous silica coatings [104]. The external silica coatings enhance the dispersion of SWCNTs, while the silica mesopores serve as a synthesis reactor for AgNPs, enabling *in situ* synthesis of AgNPs embedded in carbon nanotubes. The antimicrobial properties of AgNPs have been extensively validated [105]. This combination of SWCNTs@mSiO_2-TSD@Ag overcomes the challenge of dispersing nanomaterials and harnesses the synergistic antimicrobial capabilities of SWCNTs and AgNPs, resulting in an effect greater than the sum of its parts. It has demonstrated remarkable antibacterial efficacy in an *in vivo* rat skin infection model and represents a safe and potent new nano platform. Similarly, Benítez-Martínez *et al.* incorporated multi-walled carbon nanotubes (MWCNT) into an interpenetrating polymer network consisting of polydimethylsiloxane (PDMS), PVA, and chitosan to create a hydrogel network that combines PDMS's elasticity with PVA's swelling capacity and chitosan's cellular adhesion properties, opening up new possibilities for tissue engineering and wound dressing [106].

4.2. Other 1D antimicrobial materials

Apart from the aforementioned carbon-based 1D nanomaterials, other 1D antimicrobial materials such as metal nanorods/nanowires are primarily utilized in composite form to achieve functionalized antimicrobials [107,108]. Studies have demonstrated that Si_3N_4 exhibits broad-spectrum antibacterial activity against various microbial strains [109,110]. Ma *et al.* incorporated different amounts of Si_3N_4 into a collagen/chitosan spinning solution and subsequently employed the solution blow spinning (SBS) technique to prepare antimicrobial fibrous silk pads containing Si_3N_4 for application in chronic wound healing treatment [111]. Electrostatic spinning technology is an essential method for fabricating medical nanofibers [112,113]. Cui *et al.* utilized electrostatic spinning technique to develop copper ion-doped SiO_2 nanofibers (SiO_2NFs). These electrospun fiber filaments exhibited smooth surfaces and displayed effective antibacterial activity against both *E. coli* and *S. aureus*, with enhanced antibacterial properties observed with increasing Cu content [114]. Interestingly, Gong *et al.*'s study discovered that salt can induce beaded nanofiber formation with uniform diameters using insect cuticle protein (CPH-2) derived from the head capsule of Ostrinia furnacalis larvae. Not only does this fiber possess remarkable antibacterial activity but it also accelerates the wound healing process [115].

5. Two-dimensional antimicrobial nanomaterials

After the discovery of C_{60} and carbon nanotubes, chemists turned their attention to 2D graphene. The successful exfoliation of a single layer of graphene in 2004 marked a significant breakthrough in the field of 2D nanomaterials [116]. Subsequently, the introduction of various 2D nanomaterials such as MXene, MoS_2 nanosheets, and black phosphorus gradually enriched the realm of 2D materials and provided new avenues for research on antibacterial materials [117,118]. Liu *et al.* conducted a comparative study on the antibacterial activity of four different graphene-based materials (graphite (Gt), graphite oxide (GtO), graphene oxide (GO), and reduced graphene oxide (rGO)) against *E. coli* [119]. The results demonstrated that GO exhibited the strongest antibacterial activity, followed by rGO, Gt, and GTO. Numerous researchers have investigated the interaction between organisms and GO which has confirmed that its antibacterial properties arise from both physical membrane stress synergy and chemical oxidative stress [120,121].

5.1. Graphene-based 1D nanomaterials

Different research teams have investigated the antibacterial properties of GO against *E. coli*. Transmission electron microscope (TEM) analysis reveals that exposure to GO nanosheets at 37 °C for 2 h causes *E. coli* cells to flatten and experience severe damage to their cell membranes, resulting in cytoplasm outflow [119,122-124]. Jian *et al.* conducted a covalent grafting reaction between polyhexamethylene guanidine hydrochloride (PHMG) and GO nanosheets (MGO), which were then incorporated into a

TPU double-layer film [125]. This reaction ensures the uniform and stable distribution of PHMG on GO, providing better dispersibility compared to scaffold materials like metal-organic framework (MOF) and SiO_2 [126,127]. The MGO-TPU double-layer membrane exhibits excellent antibacterial effects and long-lasting antibacterial properties due to the combined effects of PHMG and GO, making it a promising candidate for wound dressings in skin wound healing applications. Zhang *et al.* incorporated graphene oxide nanosheets into a PVA electrospinning solution [128]. The addition of GO enhances the mechanical properties and drug loading capacity of the electrospun scaffold while also imparting certain antibacterial properties, thereby improving wound repair efficiency in rat models. Xu *et al.*, on the other hand, incorporated 2D reduced graphene oxide nanosheets modified with AgNPs into thermally responsive hydrogels [129]. This composite hydrogel can be cross-linked *in situ* form a wound dressing. This unique composite hydrogel could be cross-linked *in situ* to form a wound dressing with excellent antibacterial properties conferred by AgNPs and graphene nanosheets. Inspired by the layered structure of pearls, Xue *et al.* developed a layered porous film composed of graphene oxide-chitosan-calcium silicate (GO-CTS-CS) [130]. This film not only possessed good tensile strength and gas permeability but also exhibited photothermal antibacterial activity *in vitro* as well as photothermal anti-tumor properties *in vivo* due to the presence of GO. Zhang *et al.* utilized electrospinning technology to coat graphene oxide-dopamine methacrylamide composite material (GO-DMA) onto nanofibers, resulting in the fabrication of PLA-GO-DMA nanofiber mats that demonstrate multiple antibacterial effects [131]. In contrast to the typical hydrophobic behavior exhibited by PLA, the incorporation of GO and hydrophilic groups imparts hydrophilicity to the composite fiber mat. Additionally, DMA functions as a bonding agent, enhancing the adhesion between PLA fibers and GO nanosheets [132-134]. This nanofiber mat demonstrates favorable antibacterial properties against both Gram-positive and Gram-negative bacteria, rendering it a promising biomaterial for tissue engineering.

Skin wounds are frequently covered by exudate, which can create a barrier for topical antibiotics to penetrate and act on the deeper layers of the wound once neutrophils are activated [135]. Additionally, high-dose intravenous antibiotic treatment carries the risk of drug resistance [136]. As an alternative approach, local wound heat treatment has been proposed as an effective method for treating bacterial infections by increasing temperature to kill bacteria without damaging normal tissue structure [137,138]. Li *et al.* developed flexible nanopatches composed of graphene precipitated onto Kapton HN polyimide foils modified with gold nanopores (K/Au NHs-rGO), which exhibit photothermal properties that enable heat-induced damage to bacteria under LED illumination and subsequent bacterial killing [139].

The combination of graphene and MOFs can integrate the antimicrobial properties of 2D materials with the structural advantages of three-dimensional (3D) materials, thereby achieving 3D antimicrobial effects [140,141]. Fan *et al.* successfully fabricated a MOF-derived 2D carbon nanosheet by combining MOF and graphene for antibacterial treatment [142]. By enriching the classic MOF structure zeolitic imidazolate frameworks-8 (ZIF-8) with Zn^{2+} ions, multiple antibacterial effects were achieved. Additionally, grafting phase transformable thermal-responsive brushes (TRB) polymer enabled the transition from a hydrophilic state to a hydrophobic state. The antibacterial ability of these carbon nanosheets was tested against *E. coli* and *S. aureus*. The results demonstrated that TRB-ZnO@G uniformly dispersed in the bacterial suspension transformed into a hydrophobic state upon near-infrared light irradiation and subsequently encapsulated bacteria within the polymer matrix, leading to their capture and elimination (Fig. 3).

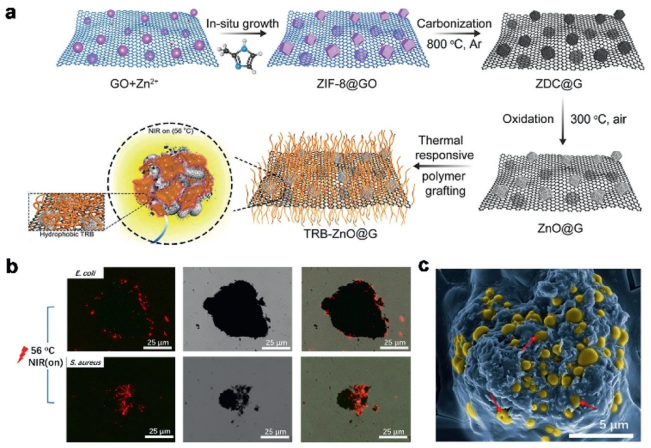

Fig. 3. (a) Schematic illustration of the TRB-ZnO@G wrapped and killed bacteria. (b) Images after a 5 min NIR irradiation. (c) SEM image for the formed TRB-ZnO@G/*S. aureus* aggregation after NIR irradiation. Copied with permission [142]. Copyright 2019, American Chemical Society.

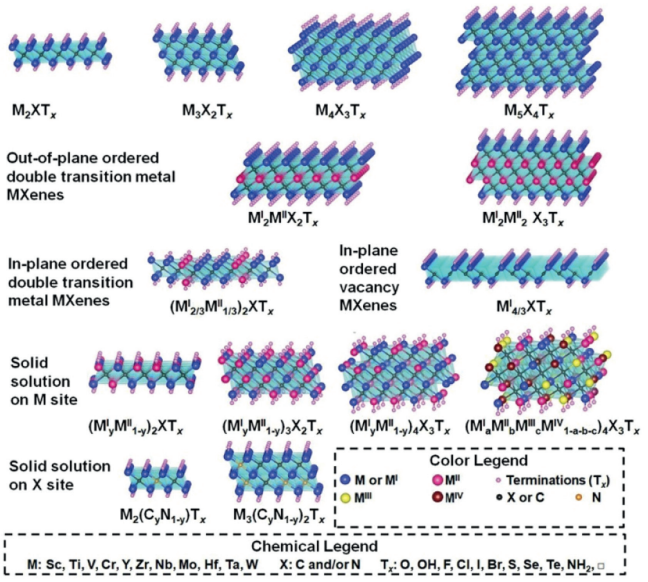

Fig. 4. Typical structure and composition of MXene. Copied with permission [118]. Copyright 2021, John Wiley and Sons.

5.2. MXenes

Graphene materials, as the largest known family of 2D materials, have been dominant in the field of 2D antimicrobial materials for years until the emergence of $M_{N+1}AX_N$ phases ($M_{N+1}AX_N$ phases). MXenes is a general term referring to 2D transition metal carbides and nitrides, which can be generally expressed by the formula $M_{n+1}X_nT_x$. Here, M represents transition metals such as Ti, X represents carbon or nitrogen, T represents functional groups like -F and -OH, and n ranges from 1 to 4 (Fig. 4) [118,143]. The components "M", "X", and "T" of MXenes consist of transition metal elements with excellent biocompatibility [144-146]. Studies have demonstrated that MXenes exhibit remarkable antibacterial properties. Zhao *et al.* synthesized ZnTi layered double hydroxide nanosheets (ZnTi-LDH) with transverse sizes ranging from 40 nm to 75 nm using the reverse microemulsion method and investigated their antimicrobial properties [147]. The experimental results demonstrated the photochemical activity of titanium-containing LDHs nanosheets. Upon exposure to visible light, the presence of these nanosheets significantly inhib-

ited the growth of *Saccharomyces cerevisiae*, *Bacillus subtilis*, and *E. coli* within 8 h. Bacterial lysis occurred due to the generation of reactive oxygen and hydroxyl radicals through photocatalysis, which attacked the membrane structure [148]. Rasool *et al.*, using SEM observation, observed severe membrane damage and cytoplasmic leakage in both *E. coli* and *Bacillus subtilis* after incubation with different concentrations of $Ti_3C_2T_x$; furthermore, separation between the cytoplasmic membrane and cell wall was evident [149].

The latest research findings by Geng *et al.* have reported the development of bio-heterojunctions ($2D^2$-bioHJs) composed of polylactic-glycolic acid (PLGA) and black phosphorus/V_2C MXene, which were prepared using electrospinning techniques [150]. These bio-heterojunctions are capable of generating a significant amount of ROS upon stimulation, effectively eliminating drug-resistant bacteria by disrupting bacterial metabolism and the electron transport chain (ETC). This macrophage-like smart nanocatalytic membrane achieves a balance between ROS generation and removal, thereby promoting skin regeneration. In another recent study conducted by Jiang *et al.*, they aimed to address the impaired immunoregulatory ability of macrophages in the high-glucose microenvironment associated with diabetes. They developed M2 macrophage exosomes (M2-Exo), which exhibited sustained-release properties and injectable characteristics when incorporated into hydrogel nanocomposites that are sensitive to heat [151]. Under conditions simulating high glucose wounds, the inclusion of MXene minimally affected the release kinetics of M2-Exo. Moreover, these composite-released M2-Exo synergistically stimulated macrophage polarization towards the M2 phenotype *in vitro* through activation of the phosphatidylinositol 3-kinase/protein kinase B (PI3K/AKT) signaling pathway. Additionally, $Ti_3C_2T_x$ MXene demonstrated anti-inflammatory and antibacterial activity that further facilitated wound healing in pityriasis cases. Huang *et al.* utilized MXene-modified polycaprolactone-MXene-chitosan-aspirin nanofibrous membranes (PCL-MX-CS-ASP) for treating refractory bacterial invasion wounds [152]. The combined antimicrobial effects of MXene, chitosan, and aspirin exhibit significant enhancement in the materials' antimicrobial activity, which is also observed even without near infrared (NIR) irradiation. Upon exposure to 808 nm NIR light, MXene's disinfectant potential is activated, leading to rapid eradication of most bacteria through photothermal and photodynamic effects.

5.3. MoS_2

Molybdenum (Mo) is a crucial trace element for living organisms [153]. In recent years, molybdenum-based materials have gained increasing usage in catalysis, electronics, and biomedicine. Clinically, molybdenum can be employed to treat Wilson's disease [154]. MoS_2 nanosheets are representative 2D transition metal chalcogenide materials that possess a sandwich structure consisting of two layers of sulfur atoms covalently bonded by S-Mo-S bonds and surrounded by a layer of metal atoms. Each layer has a thickness of 6–7 Å [154,155]. Studies have demonstrated the effective bactericidal properties of single-layered 2D MoS_2 nanosheets and chemically exfoliated MoS_2 nanosheets (ce-MoS_2) as photothermal agents [156-158]. Kumari *et al.* successfully precipitated copper peroxide nanodots (CP-nanodots) onto the surface of 2D MoS_2 nanosheets [159]. The presence of Cu^{2+} induces bacterial death through Fenton chemical decomposition of hydrogen peroxide into -OH radicals. Additionally, the photothermal effect generated by MoS_2 nanosheets synergistically enhances antimicrobial activity under near-infrared irradiation, resulting in composites with excellent broad-spectrum antimicrobial ability. Ding *et al.* utilized a microfluidic *in situ* 3D printing strategy to print hydrogel scaffolds containing MoS_2 nanosheets using a hybrid precursor solution composed of dextran polymers functionalized with benzaldehyde and cyanoacetic acid groups (DEX-BA and DEX-CA) as ink material [160]. It was demonstrated that the presence of weakly basic MoS_2 nanosheets significantly enhanced the reaction between DEX-BA and DEX-CA moieties, thereby accelerating the gelation rate of the hydrogels. The incorporation of MoS_2 nanosheets not only improved the mechanical properties but also endowed the hydrogel scaffolds with excellent *in vitro* antimicrobial ability, owing to their remarkable photothermal capability. The hydrogel (DEM) containing 1 mg/mL MoS_2 exhibited a temperature increase of 26 °C under NIR irradiation, compared to only 2 °C for blank hydrogels. The results from their antimicrobial tests revealed that upon NIR irradiation-induced temperature elevation, most bacteria co-cultured within the hydrogel were eradicated due to thermal effects.

5.4. Black phosphorus (BP)

Black phosphorus nanosheets (BPNSs), which were first isolated from bulk black phosphorus in 2014, have emerged as a prominent contender among 2D nanomaterials following the footsteps of graphene [161,162]. Similar to other 2D nanomaterials, BP exhibits remarkable antimicrobial ability due to its photothermal effect. However, what sets BP apart is its high structural anisotropy and bandgap-dependent semiconducting properties, resulting in elevated extinction coefficients and enhanced photothermal conversion efficiencies. These distinctive characteristics position it as a promising biomedical research material with immense potential [163-167]. Sun *et al.* conducted a comparative study on the antibacterial properties of BP, graphene, and MoS_2 and found that BP demonstrated superior antimicrobial efficiency while exhibiting minimal cytotoxicity [165].

After just 10 years of development, BP has emerged as a crucial component in the realm of 2D antimicrobial materials. However, its susceptibility to decomposition upon exposure to air or water significantly hampers its potential applications [166]. Fortunately, after several years of dedicated research, this issue has been gradually addressed. Numerous researchers have successfully prepared stable single-layer nanosheets of BP [168-172]. Ouyang *et al.* achieved the preparation of BP with an average size of 180 nm, which was then combined with a fibrinogen solution and a thrombin solution to create a material that could be conveniently sprayed onto diabetic wounds as an *in situ* cross-linked gel (BP@Gel) [173]. The quantitative results obtained from *S. aureus* antibacterial experiments demonstrated that approximately 94.3% of bacteria were eradicated following treatment with BP@Gel under near-infrared laser irradiation. This *in situ* spray hydrogel composed of BP@Gel proved effective in providing on-demand pain relief and antimicrobial functionality for promoting the healing process of diabetic wounds in mice (Fig. 5). Photodynamic therapy (PDT) stands out as one anti-infective treatment method; however, its effectiveness is greatly influenced by limited oxygen supply and persistence over time. To enhance PDT efficacy, Ran *et al.* employed Pt nanoparticles along with aminobenzyl-2-pyridone (APy)-decorated black phosphorus (BP@APy-Pt) as photosensitizers [174]. The Pt nanoparticles catalyzed the stabilized production of $^1O_2$ from H_2O_2, while BP@APy facilitated the storage and sustained release of O_2, inhibiting bacterial growth. Liang *et al.* developed AgNPs-loaded BPNSs as a synergistic photocatalytic disinfectant for bacterial infections by destroying bacterial cell walls/membranes and achieving enhanced antibacterial efficiency through photothermal effect after light irradiation [164]. Similarly, Zheng *et al.* integrated BPNPs-triggered PTT with antibacterial drug physcion (Phy) to create a degradable and biocompatible photothermal antibacterial material that avoids damage to normal tissues caused by higher temperatures [175].

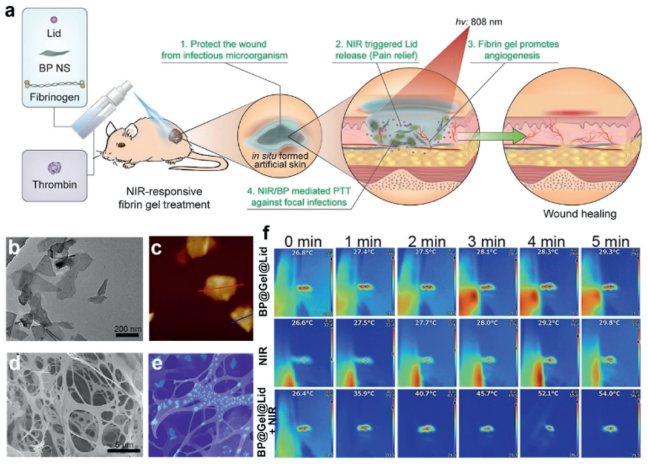

Fig. 5. (a) Schematic illustration of *in situ* sprayed NIR-responsive, pain-relieving gel for accelerated wound healing. (b) TEM image and (c) AFM image of BP NSs. (d) SEM image and (e) *Pseudo*-color SEM image of BP@Gel. (f) Photothermal image of mice feet with different treatments. Copied with permission [173]. Copyright 2020, the National Academy of Sciences.

6. Conclusions and future perspectives

As traditional antibiotics face a period of stagnation in their development, nanomaterials engineering offers a new direction for antibacterial medicine. From zero-dimensional (0D) and 1D to multidimensional nano-antimicrobial materials, the advancement of novel antimicrobial materials continues unabated. This review focuses on 0D, 1D, and 2D nanomaterials, highlighting their distinct characteristics resulting from variations in size and morphology. It also introduces the diverse antimicrobial mechanisms of nanomaterials and recent research advancements in low-dimensional nanomaterials for wound healing applications.

Overall, nano-antimicrobial materials of different dimensions possess unique attributes due to their varying sizes and morphologies. The development and application of antimicrobial nanomaterials have progressed positively. In addition to the inherent antimicrobial properties of these materials themselves, novel synergistic strategies such as acoustic dynamic antimicrobial techniques, PTT and PDT have been employed to enhance the effectiveness and broaden the application range of nanomaterials. In recent years, researchers have also begun exploring 3D and four-dimensional (4D) antimicrobial scaffolds with dynamic adaptive capabilities like antimicrobial MOFs. In the digital era, the introduction of time scales and structural dynamics is of great importance to materials science.

While the current progress in nano-antibacterial wound dressings is promising, there still exists a considerable journey ahead for scientists aspiring to transition towards clinical applications. Firstly, achieving a delicate balance between antibacterial efficacy and biocompatibility presents a formidable challenge. The clinical utilization of antibiotics necessitates stringent safety requirements for human metabolism. Therefore, the instability and potential adverse effects of nanomaterials within living organisms require further investigation. Secondly, addressing bacterial infections often involves treating mixed infections caused by multiple strains of bacteria. Many nanomaterials exhibit antibacterial effects against only one or limited number of bacteria at concentrations deemed safe for use; thus failing to meet the performance criteria for combating mixed infections with various bacterial strains, particularly fungal infections. Lastly, apart from considering nanomaterial properties, antimicrobial applications also need to encompass factors such as cost-effectiveness, reproducibility in production processes, and environmental sustainability. Overall, substantial potential remains untapped for advancing and harnessing the capabilities of antibacterial nanomaterials in wound dressing applications.

Declaration of competing interest

The authors declare that they have no known competing financial interests or personal relationships that could have appeared to influence the work reported in this paper.

CRediT authorship contribution statement

Yunfen Gao: Writing – original draft, Data curation. **Liying Wang:** Writing – review & editing, Funding acquisition. **Chufan Zhou:** Validation, Data curation. **Yi Zhao:** Writing – review & editing, Resources. **Hai Huang:** Supervision. **Jun Wu:** Supervision, Resources, Project administration, Funding acquisition.

Acknowledgments

This work was financially supportsed by National Natural Science Foundation of China (No. 52173150), Guangzhou Science and Technology Program City-University Joint Funding Project (No. 2023A03J0001), Postdoctoral Science Foundation (No. 2022M723670).

References

[1] C. Vepari, D.L. Kaplan, Prog. Polym. Sci. 32 (2007) 991–1007.
[2] G.H. Altman, F. Diaz, C. Jakuba, et al., Biomaterials 24 (2003) 401–416.
[3] R.L. Horan, K. Antle, A.L. Collette, et al., Biomaterials 26 (2005) 3385–3393.
[4] A.I. Neto, H.J. Meredith, C.L. Jenkins, J.J. Wilker, J.F. Mano, RSC Adv. 3 (2013) 9352–9356.
[5] M. Krogsgaard, V. Nue, H. Birkedal, Chemistry 22 (2016) 844–857.
[6] J. Sun, C. Su, X. Zhang, et al., Langmuir 31 (2015) 5147–5154.
[7] G.V. Vimbela, S.M. Ngo, C. Fraze, L. Yang, D.A. Stout, Int. J. Nanomed. 12 (2017) 3941–3965.
[8] T.P. Van Boeckel, S. Gandra, A. Ashok, et al., Lancet Infect. Dis. 14 (2014) 742–750.
[9] WHO, 2021. https://www.who.int/zh/news-room/fact-sheets/detail/antimicrobial-resistance.
[10] T. Verma, A. Aggarwal, S. Singh, S. Sharma, S.J. Sarma, J. Mol. Struct. 1248 (2022) 131380.
[11] D.M. Livermore, J. Antimicrob. Chemother. 64 (2009) 29–36.
[12] R. Laxminarayan, P. Matsoso, S. Pant, et al., Lancet 387 (2016) 168–175.
[13] R. Laxminarayan, Z.A. Bhutta, Lancet Global Health 4 (2016) e676–e677.
[14] V.M. D'Costa, C.E. King, L. Kalan, et al., Nature 477 (2011) 457–461.
[15] A. Upadhayay, J. Ling, D. Pal, et al., Drug Resist. Updat. 66 (2023) 100890.
[16] M. Rhouma, J.-Y. Madec, R. Laxminarayan, Int. J. Antimicrob. Agents 61 (2023) 106713.
[17] N. Guo, Y. Xia, Y. Duan, et al., Chin. Chem. Lett. 34 (2023) 107542.
[18] L. Guo, W. Kong, Y. Che, et al., Int. J. Biol. Macromol. 261 (2024) 129799.
[19] P. Kumar, P. Huo, R. Zhang, B. Liu, Nanomaterials 9 (2019) 737.
[20] W. Su, X. Luo, P. Li, et al., Chin. Chem. Lett. 35 (2024) 109522.
[21] A.J. Huh, Y.J. Kwon, J. Control. Release 156 (2011) 128–145.
[22] A. Gupta, S. Mumtaz, C.H. Li, I. Hussain, V.M. Rotello, Chem. Soc. Rev. 48 (2019) 415–427.
[23] L. Ye, Z. Cao, X. Liu, et al., J. Alloys Compd. 904 (2022) 164091.
[24] P. Makvandi, C.Y. Wang, E.N. Zare, et al., Adv. Funct. Mater. 30 (2020) 1910021.
[25] Q. Song, S.Y. Chan, Z. Xiao, et al., Prog. Org. Coat. 188 (2024) 108214.
[26] A. Arabi Shamsabadi, B. Anasori, M. Soroush, ACS Sustain, Chem. Eng. 6 (2018) 16586–16596.
[27] N. Talebian, S.M. Amininezhad, M. Doudi, J. Photochem. Photobiol. B: Biol. 120 (2013) 66–73.
[28] H. Li, M. Mu, B. Chen, et al., Mater. Res. Lett. 12 (2024) 67–87.
[29] P. Li, L. Sun, S. Xue, et al., SmartMat 3 (2022) 226–248.
[30] A. Abbaszadegan, Y. Ghahramani, A. Gholami, et al., J. Nanomater. 2015 (2015) 720654.
[31] S. Ghosh, S. Patil, M. Ahire, et al., Int. J. Nanomed. 7 (2012) 483–496.
[32] L.B. Capeletti, L.F. de Oliveira, K.d.A. Gonçalves, et al., Langmuir 30 (2014) 7456–7464.
[33] R. Kügler, O. Bouloussa, F. Rondelez, Microbiology 151 (2005) 1341–1348.
[34] T.C. Dakal, A. Kumar, R.S. Majumdar, V. Yadav, Front. Microbiol. 7 (2016) 1831.
[35] Y.H. Hsueh, K.S. Lin, W.J. Ke, et al., PLoS One 10 (2015) e0144306.
[36] G. Franci, A. Falanga, S. Galdiero, et al., Molecules 20 (2015) 8856–8874.
[37] S.S. Garg, R. Dubey, S. Sharma, A. Vyas, J. Gupta, Int. J. Biol. Macromol. 247 (2023) 125636.
[38] Y. Du, T. Li, Y. Wan, P. Liao, Crit. Rev. Eukaryotic Gene Express 24 (2014) 117–132.

[39] D. Paul, J. Gopal, M. Kumar, M. Manikandan, Chem. Biol. Interact. 280 (2018) 86–98.
[40] M. Zhang, K. Zhang, B. De Gusseme, W. Verstraete, R. Field, Biofouling 30 (2014) 347–357.
[41] D. Ravindran, S. Ramanathan, K. Arunachalam, et al., J. Appl. Microbiol. 124 (2018) 1425–1440.
[42] Y. Gao, W. Wu, K. Qiao, et al., Water Res. 204 (2021) 117603.
[43] M.K. Rai, S.D. Deshmukh, A.P. Ingle, A.K. Gade, J. Appl. Microbiol. 112 (2012) 841–852.
[44] B. Zhao, H. Wang, W. Dong, et al., J. Nanobiotechnol. 18 (2020) 59.
[45] Z. Zhou, B. Li, X. Liu, et al., ACS Appl. Bio Mater. 4 (2021) 3909–3936.
[46] Y.N. Slavin, J. Asnis, U.O. Häfeli, H. Bach, J. Nanobiotechnol. 15 (2017) 65.
[47] M.R. Hamblin, Curr. Opin. Microbiol. 33 (2016) 67–73.
[48] N. Kashef, M.R. Hamblin, Drug Resist. Updat. 31 (2017) 31–42.
[49] T. Dai, Y.Y. Huang, M.R. Hamblin, Photodiagn. Photodyn. Ther. 6 (2009) 170–188.
[50] Z. Oruba, P. Łabuz, W. Macyk, M. Chomyszyn-Gajewska, Photodiagn. Photodyn. Ther. 12 (2015) 612–618.
[51] L. Zhou, Y. Deng, Y. Ren, et al., Chem. Eng. J. 482 (2024) 148978.
[52] W. Zhang, Y. Li, J. Niu, Y. Chen, Langmuir 29 (2013) 4647–4651.
[53] J.Y. Mao, D. Miscevic, B. Unnikrishnan, et al., J. Colloid Interface Sci. 608 (2022) 1813–1826.
[54] X.L. Hu, Y. Shang, K.C. Yan, et al., J. Mater. Chem. B 9 (2021) 3640–3661.
[55] Z. Wang, T. Hu, R. Liang, M. Wei, Front. Chem. 8 (2020) 320.
[56] J.J. Liang, Y.Y. Zhou, J. Wu, Y. Ding, Curr. Drug Metab. 15 (2014) 620–631.
[57] W. Heni, X. Zejun, L. Qing, W. Jun, Eng. Regener. 2 (2021) 137–153.
[58] L. Wang, X. Huang, X. You, et al., Signal Transduction Targeted Ther. 5 (2020) 196.
[59] M.K. Ahmed, A.M. Moydeen, A.M. Ismail, et al., J. Mol. Struct. 1225 (2021) 129138.
[60] M.A. Norouzi, M. Montazer, T. Harifi, P. Karimi, Polym. Test. 93 (2021) 106914.
[61] T. Kuang, L. Deng, S. Shen, et al., Chin. Chem. Lett. 34 (2023) 108584.
[62] A.U. Khan, A.U. Khan, B. Li, et al., Photodiagn. Photodyn. Ther. 31 (2020) 101814.
[63] Q.L. Feng, J. Wu, G.Q. Chen, et al., J. Biomed. Mater. Res. 52 (2000) 662–668.
[64] K. Tahir, S. Nazir, B. Li, et al., J. Photochem. Photobiol. B: Biol. 153 (2015) 261–266.
[65] T. Xia, M. Kovochich, J. Brant, et al., Nano Lett. 6 (2006) 1794–1807.
[66] Y. Ma, C. Liu, D. Qu, et al., Biomed. Pharmacother. 89 (2017) 351–357.
[67] U.S. Malik, Q. Duan, M.B.K. Niazi, et al., Chin. Chem. Lett. 34 (2023) 108071.
[68] M. Zhou, F. Lin, W. Li, et al., Int. J. Biol. Macromol. 166 (2021) 1335–1351.
[69] A. Amirsadeghi, A. Jafari, S.S. Hashemi, et al., Mater. Today Commun. 27 (2021) 102225.
[70] K. Zheng, M.I. Setyawati, D.T. Leong, J. Xie, Nano Res. 14 (2021) 1026–1033.
[71] K. Zheng, J. Xie, ACS Nano 14 (2020) 11533–11541.
[72] S. Li, Z. Li, Q. Hao, et al., Chin. Chem. Lett. 35 (2024) 108636.
[73] L. Zhou, K. Yu, F. Lu, et al., J. Cleaner Prod. 243 (2020) 118604.
[74] Y. Zou, R. Xie, E. Hu, et al., Int. J. Biol. Macromol. 148 (2020) 921–931.
[75] K. Yi, Y. Yu, L. Fan, et al., Aggregate (2024) e509.
[76] M.S. Agren, M. Chvapil, L. Franzen, J. Surg. Res. 50 (1991) 101–105.
[77] M.S. Agren, T.A. Soderberg, C.O. Reuterving, G. Hallmans, I. Tengrup, Eur. J. Surg. 157 (1991) 97–101.
[78] G. Rath, T. Hussain, G. Chauhan, T. Garg, A.K. Goyal, Mater. Sci. Eng. C: Mater. Biol. Appl. 58 (2016) 242–253.
[79] J.P. Chen, G.Y. Chang, J.K. Chen, Colloids Surf. A 313 (2008) 183–188.
[80] R. Herrmann, F. Javier Garcia-Garcia, A. Reller, Beilstein J. Nanotechnol. 5 (2014) 2007–2015.
[81] M. Salavati-Niasari, F. Davar, Z. Fereshteh, Chem. Eng. J. 146 (2009) 498–502.
[82] A. Buzarovska, S. Dinescu, A.D. Lazar, et al., Mater. Sci. Eng. C: Mater. Biol. Appl. 104 (2019) 109893.
[83] M.K. Haider, A. Ullah, M.N. Sarwar, et al., Int. J. Biol. Macromol. 173 (2021) 315–326.
[84] Z. Sadat, F. Farrokhi-Hajiabad, F. Lalebeigi, et al., Biomater. Sci. 10 (2022) 6911–6938.
[85] K. Nishshankage, A.B. Fernandez, S. Pallewatta, P.K.C. Buddhinie, M. Vithanage, Biochar 6 (2024) 2.
[86] L. Đorđević, F. Arcudi, M. Cacioppo, M. Prato, Nat. Nanotechnol. 17 (2022) 112–130.
[87] L. Đorđević, F. Arcudi, M. Prato, Nat. Protoc. 14 (2019) 2931–2953.
[88] Q. Zeng, T. Feng, S. Tao, S. Zhu, B. Yang, Light Sci. Appl. 10 (2021) 142.
[89] M.H. Chan, R.S. Liu, M. Hsiao, Nanoscale 11 (2019) 14993–15003.
[90] D. Zhao, R. Zhang, X. Liu, et al., Nanotechnology 32 (2021) 155101.
[91] H. Wang, F. Lu, C. Ma, et al., J. Mater. Chem. B 9 (2021) 125–130.
[92] H.H. Ran, X. Cheng, Y.W. Bao, et al., J. Mater. Chem. B 7 (2019) 5104–5114.
[93] S. Pandiyan, L. Arumugam, S.P. Srirengan, et al., ACS Omega 5 (2020) 30363–30372.
[94] L. Yang, Y. An, D. Xu, et al., Small 20 (2024) 2309293.
[95] F. Cui, L. Xi, D. Wang, et al., Coord. Chem. Rev. 497 (2023) 215457.
[96] Z. Bian, A. Wallum, A. Mehmood, et al., ACS Nano 17 (2023) 22788–22799.
[97] H. Li, J. Huang, Y. Song, et al., ACS Appl. Mater. Interfaces 10 (2018) 26936–26946.
[98] F. Cui, J. Sun, J. Ji, et al., J. Hazard. Mater. 406 (2021) 124330.
[99] K. Zheng, Y. Tong, S. Zhang, et al., Adv. Funct. Mater. 31 (2021) 2102599.
[100] W.K. Boyes, C. van Thriel, Chem. Res. Toxicol. 33 (2020) 1121–1144.
[101] L. Qin, P. Wang, Y. Guo, C. Chen, M. Liu, Adv. Sci. 2 (2015) 1500134.
[102] M. Llorens-Gámez, B. Salesa, Á. Serrano-Aroca, Int. J. Biol. Macromol. 151 (2020) 499–507.
[103] M.S. Islam, A.N. Naz, M.N. Alam, A.K. Das, J.H. Yeum, Colloid Interface Sci. Commun. 35 (2020) 100247.
[104] Y. Zhu, J. Xu, Y. Wang, et al., Nano Res. 13 (2020) 389–400.
[105] M.S. Islam, J.H. Yeum, Colloids Surf. A 436 (2013) 279–286.
[106] J. Chen, X. Zhao, L. Qiao, et al., Adv. Healthc. Mater. 13 (2024) 2303157.
[107] Y. Wang, R. Cao, C. Wang, et al., Adv. Funct. Mater. 33 (2023) 2214388.
[108] Z. Zheng, W. Liang, R. Lin, et al., Small Struct. 4 (2023) 2200291.
[109] G. Pezzotti, F. Boschetto, E. Ohgitani, et al., Mater. Today Bio 12 (2021) 100144.
[110] G. Pezzotti, ACS Appl. Mater. Interfaces 11 (2019) 26619–26636.
[111] P. Ma, C.Y. Yang, C. Li, et al., Adv. Fiber Mater. 6 (2024) 543–560.
[112] H. Wu, J. Fan, C.C. Chu, J. Wu, J. Mater. Sci. Mater. Med. 21 (2010) 3207–3215.
[113] H. Zhong, J. Huang, J. Wu, J. Du, Nano Res. 15 (2022) 787–804.
[114] J. Cui, Y. Cai, X. Yu, et al., Adv. Fiber Mater. 6 (2024) 278–296.
[115] Q. Gong, B. Liu, F. Yuan, et al., ACS Nano 17 (2023) 23679–23691.
[116] K.S. Novoselov, A.K. Geim, S.V. Morozov, et al., Science 306 (2004) 666–669.
[117] X. He, S. Koo, E. Obeng, et al., Coord. Chem. Rev. 492 (2023) 215275.
[118] M. Naguib, M.W. Barsoum, Y. Gogotsi, Adv. Mater. 33 (2021) 2103393.
[119] S. Liu, T.H. Zeng, M. Hofmann, et al., ACS Nano 5 (2011) 6971–6980.
[120] X. Qiu, X. You, X. Chen, et al., Int. J. Nanomed. 12 (2017) 4349–4360.
[121] T. Pulingam, K.L. Thong, J.N. Appaturi, et al., Eur. J. Pharm. Sci. 142 (2020) 105087.
[122] Y. Tu, M. Lv, P. Xiu, et al., Nat. Nanotechnol. 8 (2013) 594–601.
[123] V.T.H. Pham, T.Vi Khanh, M.D.J. Quinn, et al., ACS Nano 9 (2015) 8458–8467.
[124] S. Wu, Y. Liu, H. Zhang, L. Lei, J. Orthop. Surg. Res. 14 (2019) 305.
[125] Z. Jian, H. Wang, M. Liu, et al., Mater. Sci. Eng. C 111 (2020) 110833.
[126] W. Shao, X. Liu, H. Min, et al., ACS Appl. Mater. Interfaces 7 (2015) 6966–6973.
[127] P. Zhang, H. Wang, X. Zhang, et al., Biomater. Sci. 3 (2015) 852–860.
[128] Q. Zhang, Q. Du, Y. Zhao, et al., RSC Adv. 7 (2017) 28826–28836.
[129] X. Yan, W.-W. Fang, J. Xue, et al., ACS Nano 13 (2019) 10074–10084.
[130] J. Xue, X. Wang, E. Wang, et al., Acta Biomater. 100 (2019) 270–279.
[131] Q. Zhang, Q. Tu, M.E. Hickey, et al., Colloids Surf. B 172 (2018) 496–505.
[132] S. Farah, D.G. Anderson, R. Langer, Adv. Drug Deliv. Rev. 107 (2016) 367–392.
[133] P. Saini, M. Arora, M.N.V.R. Kumar, Adv. Drug Deliv. Rev. 107 (2016) 47–59.
[134] Y. Ramot, M. Haim-Zada, A.J. Domb, A. Nyska, Adv. Drug Deliv. Rev. 107 (2016) 153–162.
[135] R. Bilyy, V. Fedorov, V. Vovk, et al., Front Immunol. 7 (2016) 424.
[136] A. MacGowan, E. Macnaughton, Medicine 45 (2017) 622–628.
[137] K. Turcheniuk, C.H. Hage, J. Spadavecchia, et al., J. Mater. Chem. B 3 (2015) 375–386.
[138] W.L. Chiang, T.T. Lin, R. Sureshbabu, et al., J. Control. Release 199 (2015) 53–62.
[139] C. Li, R. Ye, J. Bouckaert, et al., ACS Appl. Mater. Interfaces 9 (2017) 36665–36674.
[140] D. Mao, F. Hu, Kenry, et al., Adv. Mater. 30 (2018) 1706831.
[141] X. Pan, L. Bai, H. Wang, et al., Adv. Mater. 30 (2018) 1800180.
[142] X. Fan, F. Yang, J. Huang, et al., Nano Lett. 19 (2019) 5885–5896.
[143] M. Naguib, O. Mashtalir, J. Carle, et al., ACS Nano 6 (2012) 1322–1331.
[144] K. Chen, N. Qiu, Q. Deng, et al., ACS Biomater. Sci. Eng. 3 (2017) 2293–2301.
[145] A.M. Jastrzębska, A. Szuplewska, T. Wojciechowski, et al., J. Hazard. Mater. 339 (2017) 1–8.
[146] H. Lin, Y. Chen, J. Shi, Adv. Sci. 5 (2018) 1800518.
[147] Y. Zhao, C.J. Wang, W. Gao, et al., J. Mater. Chem. B 1 (2013) 5988–5994.
[148] Y. Li, W. Zhang, J. Niu, Y. Chen, ACS Nano 6 (2012) 5164–5173.
[149] K. Rasool, M. Helal, A. Ali, et al., ACS Nano 10 (2016) 3674–3684.
[150] C. Geng, S. He, S. Yu, et al., Adv. Mater. 36 (2024) 2310599.
[151] X. Jiang, J. Ma, K. Xue, et al., ACS Nano 18 (2024) 4269–4286.
[152] Y. Huang, S. He, S. Yu, et al., Small 20 (2024) 2304119.
[153] J.A. Novotny, C.A. Peterson, Adv. Nutr. 9 (2018) 272–273.
[154] S. Manzeli, D. Ovchinnikov, D. Pasquier, O.V. Yazyev, A. Kis, Nat. Rev. Mater. 2 (2017) 17033.
[155] J. Liao, L. Wang, S. Ding, et al., Nano Today 50 (2023) 101875.
[156] X. Yang, J. Li, T. Liang, et al., Nanoscale 6 (2014) 10126–10133.
[157] C. Liu, D. Kong, P.C. Hsu, et al., Nat. Nanotechnol. 11 (2016) 1098–1104.
[158] F. Cao, L. Zhang, H. Wang, et al., Angew. Chem. Int. Ed. 58 (2019) 16236–16242.
[159] A. Kumari, J. Sahoo, M. De, Nanoscale 15 (2023) 19801–19814.
[160] X. Ding, Y. Yu, W. Li, Y. Zhao, Matter 6 (2023) 1000–1014.
[161] L. Zhang, J. You, H. Lv, et al., Int. J. Nanomed. 18 (2023) 6563–6584.
[162] M. Qiu, W.X. Ren, T. Jeong, et al., Chem. Soc. Rev. 47 (2018) 5588–5601.
[163] X. Bai, R. Wang, X. Hu, et al., ACS Nano 18 (2024) 3553–3574.
[164] M. Liang, M. Zhang, S. Yu, et al., Small 16 (2020) 1905938.
[165] Z. Sun, Y. Zhang, H. Yu, et al., Nanoscale 10 (2018) 12543–12553.
[166] S. Anju, J. Ashtami, P.V. Mohanan, Mater. Sci. Eng. C: Mater. Biol. Appl. 97 (2019) 978–993.
[167] Y. Xu, S. Chen, Y. Zhang, et al., J. Mater. Chem. B 11 (2023) 7069–7093.
[168] J. Kang, J.D. Wood, S.A. Wells, et al., ACS Nano 9 (2015) 3596–3604.
[169] C. Sun, L. Wen, J. Zeng, et al., Biomaterials 91 (2016) 81–89.
[170] Z. Wu, T. Huang, G. Sathishkumar, et al., Adv. Healthcare Mater. 13 (2024) 2302058.
[171] M. Fortin-Deschênes, F. Xia, Nat. Mater. 22 (2023) 681–682.
[172] C. Xie, Y. Xu, Y. Liu, et al., Chem. Eng. J. 477 (2023) 146997.
[173] J. Ouyang, X. Ji, X. Zhang, et al., Appl. Biol. Sci. 117 (2020) 28667–28677.
[174] P. Ran, W. Chen, H. Zheng, et al., Nanoscale 13 (2021) 13506–13518.
[175] H. Zheng, H. Li, H. Deng, et al., Colloids Surf. B 214 (2022) 112433.